Article:
Hu, Z, Nourafkan, E, Gao, H et al. (1 more author) (2017) Microemulsions stabilized by in-situ synthesized nanoparticles for enhanced oil recovery. Fuel, 210. pp. 272-281. ISSN 0016-2361

https://doi.org/10.1016/j.fuel.2017.08.004

Microemulsions stabilized by in-situ synthesized nanoparticles for enhanced oil recovery

Zhongliang Hu[1], Ehsan Nourafkan[1], Hui Gao[1], Dongsheng Wen[2,1,*]

[1]School of Chemical and Process Engineering, University of Leeds, Leeds, LS2 9JT, UK

[2]School of Aeronautic Science and Engineering, Beihang University, Beijing, 100191, China

Abstract

Nanoparticles (NPs) have been recently proposed to stabilize microemulsions (MEs) to improve their stability under harsh conditions, i.e. high temperature and high salinity as in hydrocarbon reservoirs. This work developed a novel method to produce iron oxide nanoparticles (IONPs) in-situ in oil-in-water (o/w) MEs, and examined their performance in improving oil recovery. IONPs were in-situ synthesized in MEs containing brine, n-hexane, mixture of SDS and Span 80 as the surfactants, and propyl alcohol as the co-solvent. The enhanced oil recovery (EOR) potentials of MEs and MEs containing different concentrations of IONPs (MEIN) were investigated in a core flooding system. The results indicated that the use of MEIN can significantly increase the oil recovery efficiency, i.e., jumping from 10% for ME without being stabilized NPs to 28.9% at a NPs concentration of 6400 ppm. Moreover, MEIN achieved much lower and more stable pressure profile (i.e. nearly one order of magnitude smaller) during the flooding and post-flooding stage, showing its excellent injection applicability. Four potential EOR mechanisms were examined and the formation of stable MEs synergistically stabilized by NPs and surfactants was considered as the main reason, supplemented by less formation of viscous phase, more stable IFT and increased viscosity for better mobility control.

Keywords: Enhanced oil recovery, microemulsion, nanoparticles, stabilization, synergistic effect

1. Introduction

The global demand of energy is expected to increase as much as 50% in the next 20 years. The era of finding "easy oil" is coming to an end, and future supply will become more reliant on hydrocarbons produced from unconventional hydrocarbon sources and enhance oil recovery (EOR) processes. It is estimated that for every barrel of oil we used today, there are still two barrels left in the reservoir. EOR techniques such as thermal, gas-injection and chemical methods are used in physical situations where conventional methods are inefficient or undesirable. Chemical EOR involve a process for the injection of surfactant, polymer, alkali or emulsion slug to reduce the interfacial tension (IFT) between oil and water phases, or/and reduce the mobility ratio between displacing fluid and hydrocarbon which consequently reduces the fluid capillary force and mobilizes the residual oil [1, 2].

Comparing to surfactant flooding, oil-in-water (o/w) emulsion flooding has some distinct advantages that could yield higher recovery rate due to the attainment of ultralow IFT and higher viscosity [3]. A few pilot tests of ME flooding were conducted [2, 4], and numerous studies have been done to assess the properties of ME, especially the effects of viscosity, surface tension and resistivity on EOR [3]. However, the stability of ME still remains as a big challenge. The o/w emulsions, which are generally stabilized by surfactants or polymers, can be degraded or deformed gradually inside reservoirs under high temperature and high salinity conditions [5, 6], and the mobility control by those surfactant-stabilized MEs is usually not satisfactory [6].

Nanoparticles (NPs) have been recently proposed to stabilize ME. Comparing to pure surfactant-stabilized ME, NPs as a stabilizer have some distinct advantages including high tolerance to temperature and salinity in reservoirs [7-9], increased conformance control [10] and reduced surfactant consumption [11, 12]. The surface wettability of nanoparticle can be tuned to generate ME droplets in desired shapes and sizes [8]. In addition, the nanoparticle can act as sensor

and carry additional functions [13-22], which can interact with the variation of temperature, pressure and specific chemicals etc. Despite that the most commonly-used particle for ME stabilization is silica [6, 9, 23-25], only a few other NPs have been reported to stabilize ME for EOR purpose, including hydrophilic silica NPs [6, 9], partially hydrophobic modified SiO_2 NPs [23], and partially hydrophobic clay particles [9]. However, it is seldom reported that magnetic NPs, whose behavior can be controlled by an external magnetic field, were applied as foam/emulsion stabilization agent for EOR applications. While some studies investigated super-/para- magnetic NPs transporting in porous media and adsorption at o/w interface [11], the focus was on the migration and deposition properties of NPs in rock samples, not for stabilizing emulsions. It is also noteworthy that among all the work published, NPs-stabilized MEs were produced in a two-step method. In this method, nanoparticles were produced first, and then mixed with CO_2 to form CO_2/water emulsions, or o/w, w/o emulsions [26-28]. For the two-step synthesis method, nanoparticles need to be prepared and stored in advance, which inevitably increased cost and produced many agglomerations. In-situ synthesis of NPs for emulsification, and in the same time improving ME stability will have important implications / promise for future chemical EOR techniques.

For ME-EOR to work, another essential aspect that needs to be considered is the pressure gradient when ME migrating in rocks matrix [29, 30]. Though extensive work has been conducted on colloidal transport for environmental considerations [31-34], the transport of ME in porous media in the presence of oil phase has been scarcely investigated to date, especially when it is stabilized by NPs. From practical considerations, it is preferable to use the ME with lower injection pressure to reduce the pump power required to push displacing fluids and hydrocarbon to production well, and prevent the formation from damaging by high pressure.

This work aims to develop a novel method to produce IONP in-situ in an o/w ME and examine the composite's potential for enhanced oil recovery. Three tasks are designed, which include, i) design and production of appropriate o/w ME at optimum salinity, ii) in-situ production of IONP inside ME prepared at optimized salinity, where IONPs were firstly demonstrated to stabilize ME and iii) core-flooding experiments to assess the performance of bare MEs and NPs-stabilized MEs, in terms of EOR efficiency and pressure drop. The results reveal that MEs stabilized by in-situ produced IONPs have great potential in increasing oil recovery efficiency while maintaining an excellent pressure profile.

2. Experimental Procedure

2.1. Materials

Analytical grade materials including n-hexane, sodium chloride, sodium hydroxide, Span 80, Sodium dodecyl sulphate (SDS) and propyl alcohol were purchased from Sigma Aldrich and used as received. The iron (III) 2-ethylhexanoate and mineral oil with a measured value of 42.6 mPa·s were obtained from Alfa Aesar and Kerax Ltd. (UK), respectively. The standard glass beads with diameter of 425-600 μm were purchased from Sigma Aldrich. Prior to use, the glass beads were thoroughly cleaned using a sequential acid wash, water rinse, ultrasonication, and oven-drying procedure [31].

2.2. Microemulsion preparation and characterization

A set of microemulsion (ME) suspensions were synthesized at various ionic strength ranging from 0 to 10 wt% NaCl. The other compositions of ME were fixed as 4 wt% n-hexane as the oil phase, 4 wt% propyl alcohol as the co-solvent, 4 wt% SDS as the surfactant, and 1% Span 80 as the co-surfactant to achieve an ultra-low interfacial tension between the oil and water phases, $\gamma_{o/w}$, where sole SDS is not sufficient to achieve due to its single-hydrocarbon-chain structure. The

optimum salinity of ME occurs when the interfacial tension (IFT) between ME and mineral oil achieves minimum value, which was measured by an optical tensiometer (KSV CAM 200, KSV instruments Ltd., Finland) under atmospheric environment. One of the advantages of using ME compared to surfactant solution is that in ME solution, surfactants can distribute at the interface between oil droplets and water phase, consequently preventing themselves from adsorbing on the substrate or forming micelles. It is commonly known that at high concentrations, the surfactant molecules tend to self-assemble and form micelles, which could precipitate on the substrate and reduce the availability of surfactant in the solution.

2.3. In-situ synthesis of Iron Oxide NPs in microemulsion

The procedures from Okoli et al. [35] and Sanchez-Dominguez et al. [36, 37] were referred and modified for the synthesis of iron oxide nanoparticle (IONP) in o/w MEs. Generally, one type of ME containing the metallic precursor and another one the precipitating agent of reaction are mixed together. Upon mixing, the collision and coalescence of droplets could allow the originally-separated reactants contacting with each other, thus chemical reaction is triggered. The surfactant-covered water droplets actually act as nanoreactor for the formation of nanoparticles. Chemical reaction in emerged droplet experiences subsequently the process of nuclei, growth and finally formation of nanoparticles, after exchanging of precursors [36].

The concentration of reactants was pre-determined so that the concentration of final IONP in ME could reach approximately 800, 1600 and 6400 ppm after the reaction. Briefly, Iron (III) 2-ethylhexanoate was firstly dissolved in oil phase and then used to formulate 20 mL ME at different salinities of 0, 5 (optimum salinity as determined in section 3.1) and 8 wt% NaCl. Sodium hydroxide with a stoichiometry value was dissolved in brine with a similar salinity so that the amount of brine for NaOH solution was considered tenth of ME. NaOH solution as a precursor was added dropwise via a syringe pump (KDS-410-CE, kdScientific, USA) to synthesize IONP in

ME, as shown in Figure 1. An ultrasound probe (Fisher scientific Ltd.) operating with an amplitude of 25 out of 100 was used for mixing and performing the proposed reaction below.

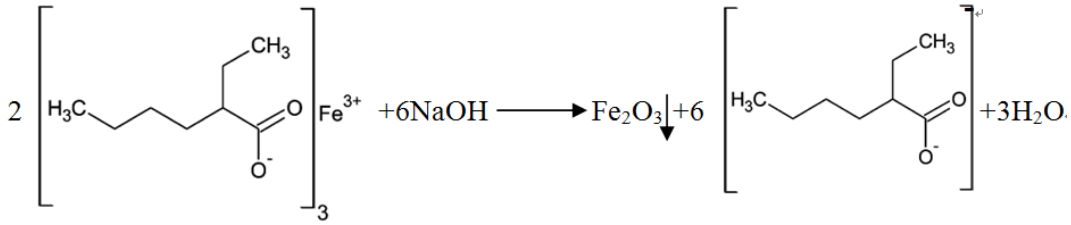

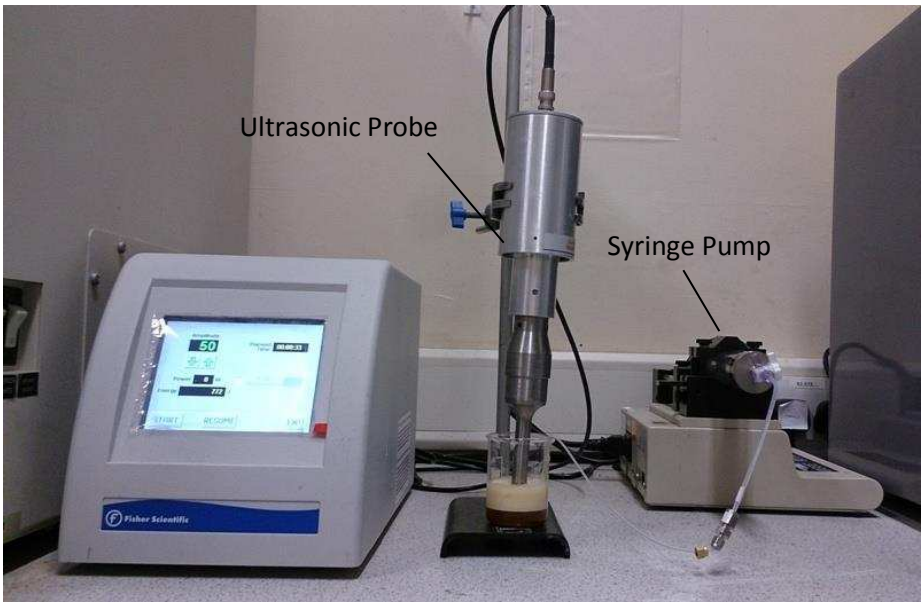

Figure 1. Experimental ultrasound sensor set-up for production iron oxide nanoparticles.

2.4. Porous medium preparation and Core-flooding Setup

The cleaned glass beads were packed into glass column via a series of strictly wet-packing procedures to make sure the geometries and hydrodynamic parameters such as porosity and permeability are relatively constant for different packing. Parameters relating to the column are listed in Table 1.

Table 1. Parameters in average value for packed glass beads column from over 20 times practice for packing.

Porous media properties	Value

Bulk volume (mL)	33.7±1.4
Pore volume (mL)	12.8±0.5
Porosity (%)	38.01±1.57
Absolute permeability (mD)	98.0±17.3
Mass of wet glass beads (g)	63.60±3.18
Mass of dry glass beads (g)	50.80±2.65
Liquid in the pore space (g)	12.8 ±0.5

A core-flooding system was set up to reveal the EOR potential for ME with in-situ synthesized IONP. Figure 2 shows the integrated experimental instruments and schematic view of the core-flooding setup. A HPLC pump (Series I, Cole-Parmer Instrument Co. Ltd.) was used for injecting brine during core flooding. A syringe pump (KDS 410, KD Scientific Inc. USA) was applied to inject mineral oil and different solutions with separate syringes in order to avoid overlap contamination. The concentration of IONPs in suspension was measured by UV-Vis spectrophotometer (UV-1800 Shimadzu). A pressure transducer (150 psi, Omega Engineering Ltd.) was used to measure the pressure drop along the packed column. The effluent liquid was collected in a 50 mL graduated cylinder marked in 0.1 mL divisions in order to determine the accumulate oil recover. The procedures of core-flooding experiments were accomplished as below:

- Brine saturation by injecting at less 20 PV of brine at optimum salinity (5 wt%) into the glass column at 2 mL /min in order to make sure the column is fully saturated by brine and allow enough time for grains depositing.
- Oil saturation by injecting mineral oil at flow rate of 0.5 mL/min until desired irreducible water saturation (S_{wi} =25%) was achieved, and the original oil in place (OOIP) is determined by the volume of water collected.

- Brine flooding as secondary oil recover stage was performed with a fixed flow rate of 0.5 mL/min for 3 PV, and followed by 20 mL (1.6 PV) displacing sample injection at a flow rate of 0.5 m/min to simulate tertiary EOR.
- Chase water injection at a flow rate of 0.5 mL/min for 20 mL.

Figure 2. Experimental core flooding set-up.

3. Results and discussion

3.1 IFT, droplet size and optimum salinity for microemulsion

As explained in section 2.2, the ME was fabricated under different salinities. The transparency of ME samples containing NaCl at 5 and 7 wt% show the formation of oil core inside ME, whereas when the amount of NaCl was lower or higher than 5 wt%, the ME was not fully formed. The oil/water phase of ME even experienced segregation with presence of 10 wt% NaCl (Figure 3). The reason behind this phenomenon is because the surfactant distribution at o/w interface can be affected by the electrolyte present in aqueous phase, which will be further explained in Figure 5. Corresponding to the macroscopic image of transparence shown in Figure 3a, the IFT results in Figure 4 consistently show that with the presence of 5 wt% of NaCl, the IFT between ME and

mineral oil was reduced most effectively to the relative low region (<0.01 mN/m) with a tiny drop hanging on the syringe tip, due to the sufficient formation of ME. By decreasing or increasing the salinity from 5 wt%, the IFT increased for both directions. Similarly, the size determined by DLS method in Figure 3b also shows the same trend with transparence and IFT. Therefore, the 5 wt% NaCl was determined as optimum salinity for ME and IONPs fabrication.

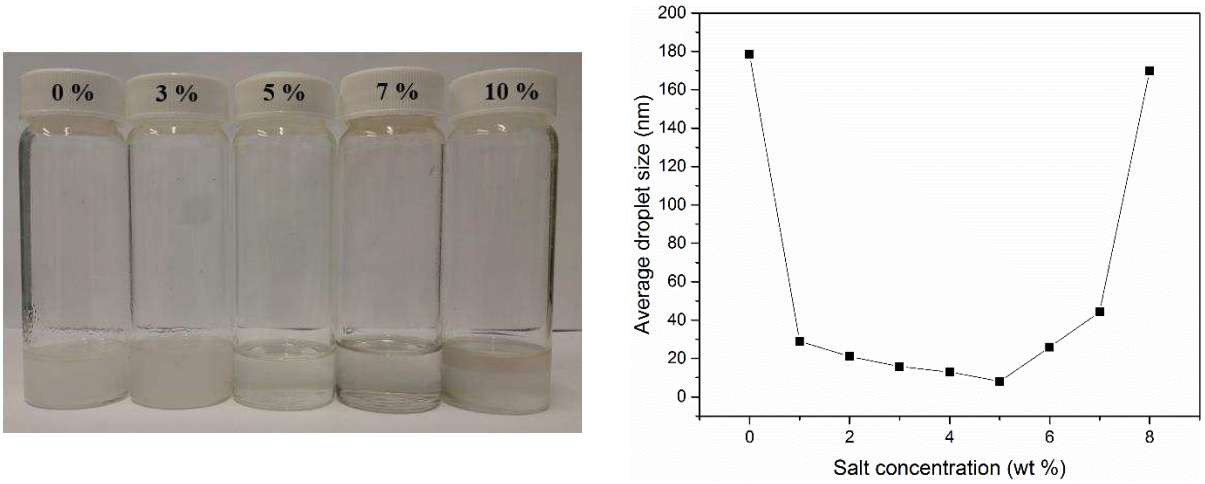

Figure 3. (a) Visualization of o/w ME samples containing NaCl from 3 wt% to 10 wt%; (b) Hydrodynamic size of ME samples with different NaCl concentrations.

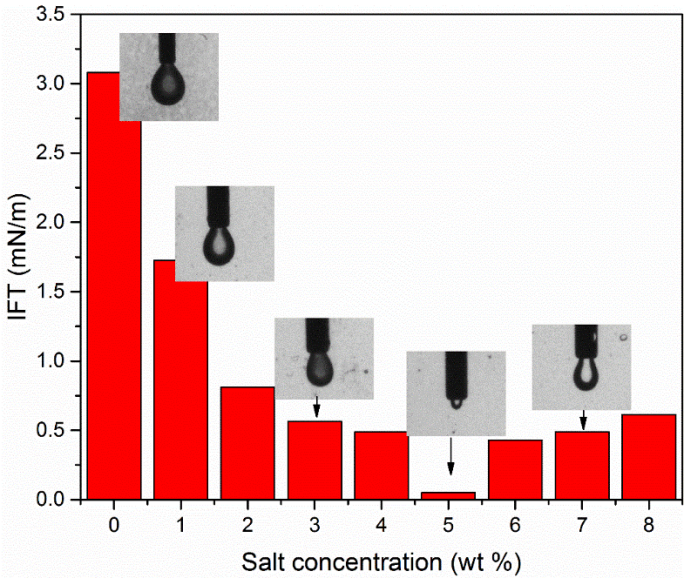

Figure 4. The IFT between ME suspension and mineral oil. Insets are images of ME suspension hanging on needle tip. The volume of ME sample capable to hang on needle tip is changing as the trend of IFT.

Increasing salinity could decrease the mutual solubility between water and surfactant. At lower salinities (e.g. <3 wt %), more surfactant molecules were dispersed in water phase. Therefore, the steric and electrostatic repulsion between oil droplets is too weak to overcome the hydrogen bonds of water molecules. As salinity increased, the solubility of surfactant in water phase is increasingly reduced and most surfactants tend to distribute at the oil/water interface, which leads to the decrease of interfacial tension and formation of oil nanodroplets. At very high salinity values (e.g. 10 wt%), the screening impact of the extra electrolytes compress the electrical double layers around droplets and the O/W phases would be separated (Figure 5).

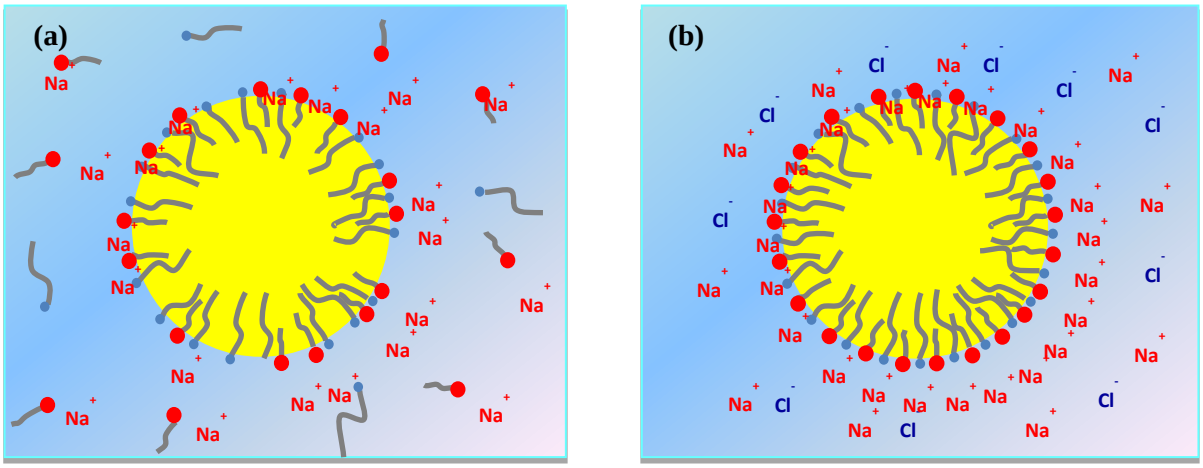

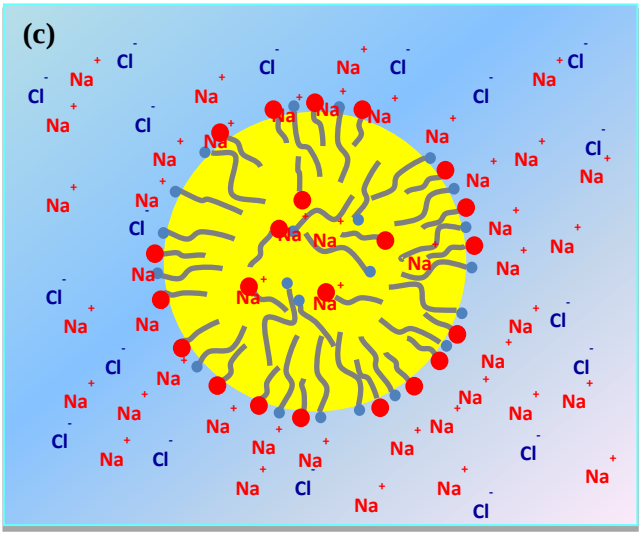

Figure 5. Schematic of surfactant distribution at the o/w interface as the increasing of ionic strength. (a) More surfactants are dispersed in water phase at low salinity water; (b) most surfactants distribute at the interface at proper salinity; (c) at high concentration of salt, the electro double layer is compressed.

3.2 Stability and morphology of composite ME

Figure 6a shows that the IONPs are successfully synthesized in ME, and they can be drawn towards a magnet (neodymium-samarium cobalt magnet with 18 kg pull force). The long-term stability was checked by unaided eye observation after synthesis of IONPs, and results in Figure 6b show that ME suspension with 5 wt% NaCl had the best macroscopic stability after 24 h. The morphologies of the synthesized IONPs were examined using a transmission electron microscope (TEM, FEI Tecnai TF20). As shown in Figure 7, the observed IONPs mainly consist of globular morphologies in the order of 5 to 20 nm.

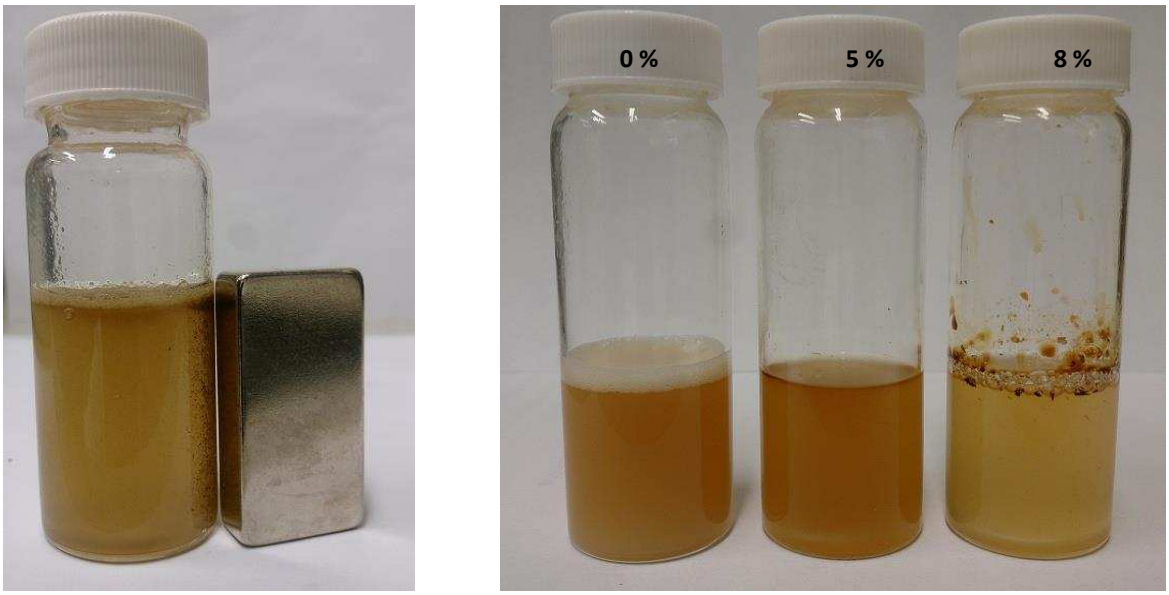

Figure 6. IONPs fabricated in O/W ME a) nanoparticle moving towards one side of bottle with presence of magnet, b) composite ME under different salinity after 24 h.

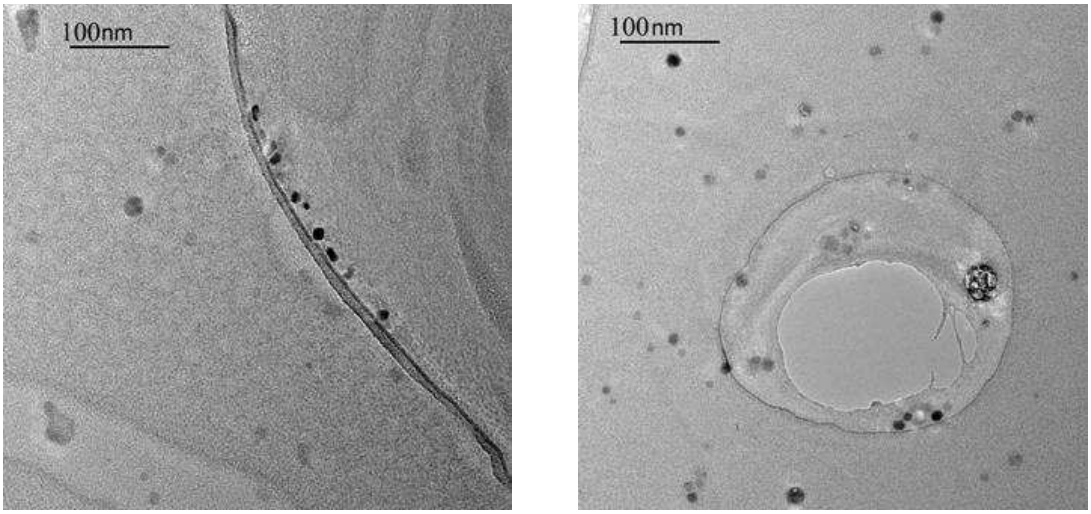

Figure 7. TEM photos of iron oxide nanoparticles which synthesized in ME at the optimum salinity.

3.3 Fluids viscosities

The dynamic viscosities of ME suspension, and ME containing in-situ synthesized IONPs (MEIN) are shown in Figure 8. Through the formation of IONPs in ME, the viscosity of the ME

is markedly influenced by the presence of both nanoparticle and surfactant. The increase in viscosity is due to that the adsorbed nanoparticle may slow down the diffusion of surfactant near o/w interface [38], and the particle-surfactant network proposed in Figure 11b also prevents the destruction and coalescence of ME when shear forces applied. Similar reports in terms of emulsion/foam viscosity increased by NPs were reported by several authors. Adsorbed nanoparticles may increase the interfacial viscosity [24, 38, 39], which may further slow lamella drainage and stabilize foam [40, 41]. It is also interesting to see that ME with 6400 ppm Fe_2O_3 NPs experienced a dramatic increase in viscosity. This suggests that when optimal amount of nanoparticles and surfactant are employed, they can favor the formation of a strong high-quality emulsion/foam, as found by Prigiobbe et al. [42]

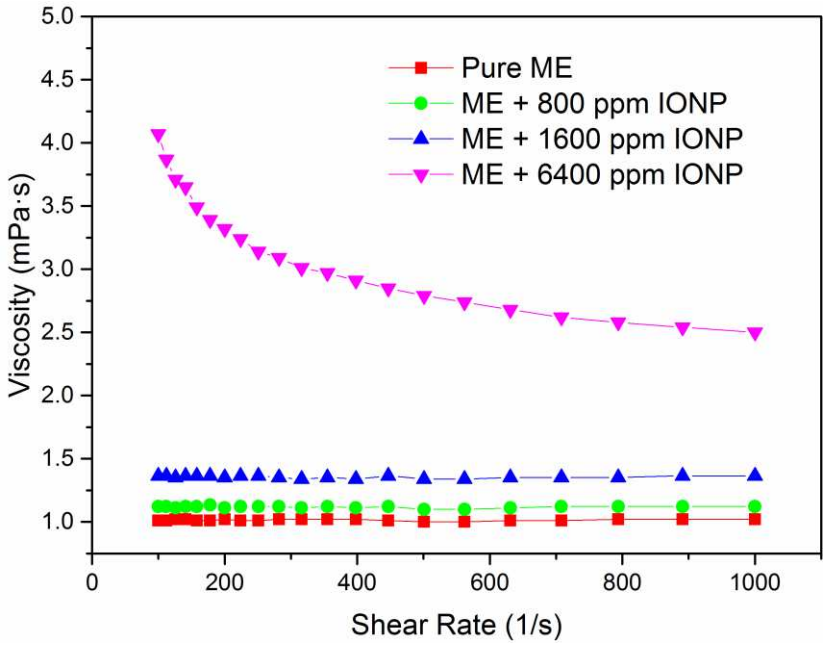

Figure 8. Viscosity of displacing samples

3.4 Oil displacement experiments

3.4.1 Oil recovery efficiency

In order to clarify the effects of nanoparticles, four tertiary flooding experiments were conducted with sole ME, and ME with in-situ formed IONPs at concentrations varying from 800

to 6400 ppm. As described in the coreflooding procedures, all the effluent materials, including oil, brine and ME suspension, were collected by using a long slim graduated tube marked in 0.1 mL divisions. Due to the density difference, the oil/water phase can be separated instantly and automatically. The cumulative oil recovery efficiency (E_{COR}) is calculated by using the amount of cumulative oil production divided by the OOIP (Original Oil in Place) at the residual water saturation (S_{wi}) of 25%. The EOR efficiency (E_{EOR}) is calculated by using the amount of oil produced in the process of ME/chase-water flooding divided by the oil left at end of brine/ME flooding.

It can be seen that the cumulative oil recovery efficiencies of brine floodings for different cases are quite close to each other (at around 45%), which means that the tertiary flooding started from the similar residual oil saturation. With an overall oil recovery efficiency of 59.1 % OOIP by the end of tertiary flooding, ME can mobilize 10% more trapped oil (EOR efficiency relative to OOIP) after brine flooding, while the presence of nanoparticles in ME further improved the efficiency, depending on the amount of IONPs contained (Figure 9). With the increase of IONPs concentration, the cumulative oil recovery efficiency was increased from 59.1% to 85.2%, and EOR efficiency was correspondingly increased from 10% to 28.9% (Table 2). In addition to a higher oil recovery ability, the pressure drop for MEIN flooding is more stable and lower than that of ME flooding, which is beneficial for the flow assurance in oil reservoir (Figure 10).

Table 2. The amount of oil recovered at different stages, for flooding experiments with different displacing fluids

Displacing fluid	E_{COR} after brine flooding, % OOIP	E_{COR} after ME flooding, % OOIP	Ultimate oil recovery efficiency % OOIP	E_{EOR} by ME, % OOIP	E_{EOR} by Chasing-water, %
ME	42.4	52.4	59.1	10.0	6.7

ME+ 800 Fe_2O_3	48.5	61.9	70.5	13.4	8.7
ME+1600 Fe_2O_3	45.9	61.6	73.1	15.7	11.5
ME+6400 Fe_2O_3	43.4	72.3	85.2	28.9	12.9

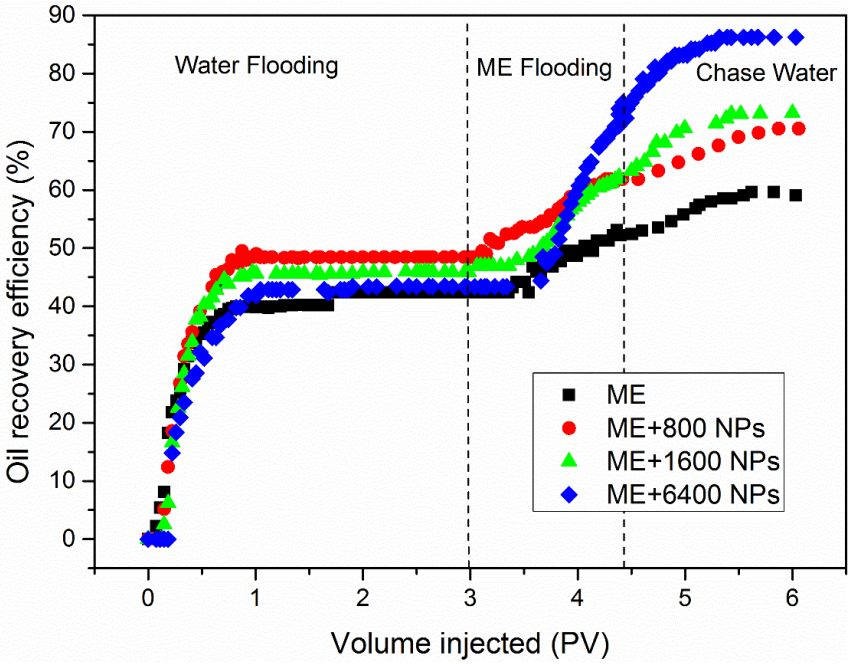

Figure 9. Tertiary oil recovery by ME and ME stabilized by in-situ synthesized Fe_2O_3 NPs.

3.4.2 Pressure files during injection

Pressure drop is necessary consideration for the design of core flooding. A 3.28 psi/m pressure gradient is common for field-scale water flooding, at the frontal velocity generally around 1 ft/day [29]. Therefore, a similar pressure gradient is necessary for the design of chemical flooding at given flow rate in laboratory. Figure 10a shows the differential pressures for the core flooding experiments, by ME and MEIN (with 800 ppm NPs) formulated with the same surfactant concentration. For ME flooding, the pressure at tertiary stage started slightly higher than that in brine flooding stage, but experienced a rapidly increase approximately from 3.5 PV, soaring up over 20 psi by the end of tertiary flooding. This might be attributed to the surfactant release trigged

by ME destruction and its retention in porous media. However, after stabilized by IONP the pressure profile for ME kept lower than 6 psi, which is even much lower than brine flooding stage and without tendency to increase, as shown in Figure 10b. The reason is because stabilized by nanoparticles, the ME structure is much more stable and there is a persistent existence of particle and surfactant molecules at the interface.

Considering the chasing-water injection processes, the pressure for MEIN was still lower than 4.5 psi and gradually declined, while the pressure for ME saw a heavy fluctuation at around 40 psi. It means that during the chasing-water injection process, ME kept destruction and released the surfactant previously distributed at the o/w interface, while the MEIN could still keep its texture synergistically stabilized by NPs and surfactant, and prevent pressure gradient from fluctuating caused by surfactant retention in porous media. The synergistic effect will be explained in detail in Section 3.4. In addition, because of the electrostatic and steric effect jointly introduced by NPs and surfactant, the ME did not tend to adsorb on the surface of glass beads, or breakup due to the collapse of interface texture (Figure 11c).

To evaluate the pressure drop and surfactant retention in glass beads matrix, we did the dynamic surfactant adsorption test by injecting surfactant and ME into the column packed with glass beads. The pressure profiles are carefully monitored and the amount of surfactant retarded in porous media was determined by sand washing method. Actually, we have injected surfactant solution and ME suspension through the column packed with both crushed sandstone and calcite limestone and without present of oil phase. Similar to Figure 10, the pressure for surfactant fluctuated more heavily than that for ME when flowing through the packed porous media without oil phase, caused by more surfactant adsorbed in porous media, which is one of the main challenges encountered by surfactant flooding.

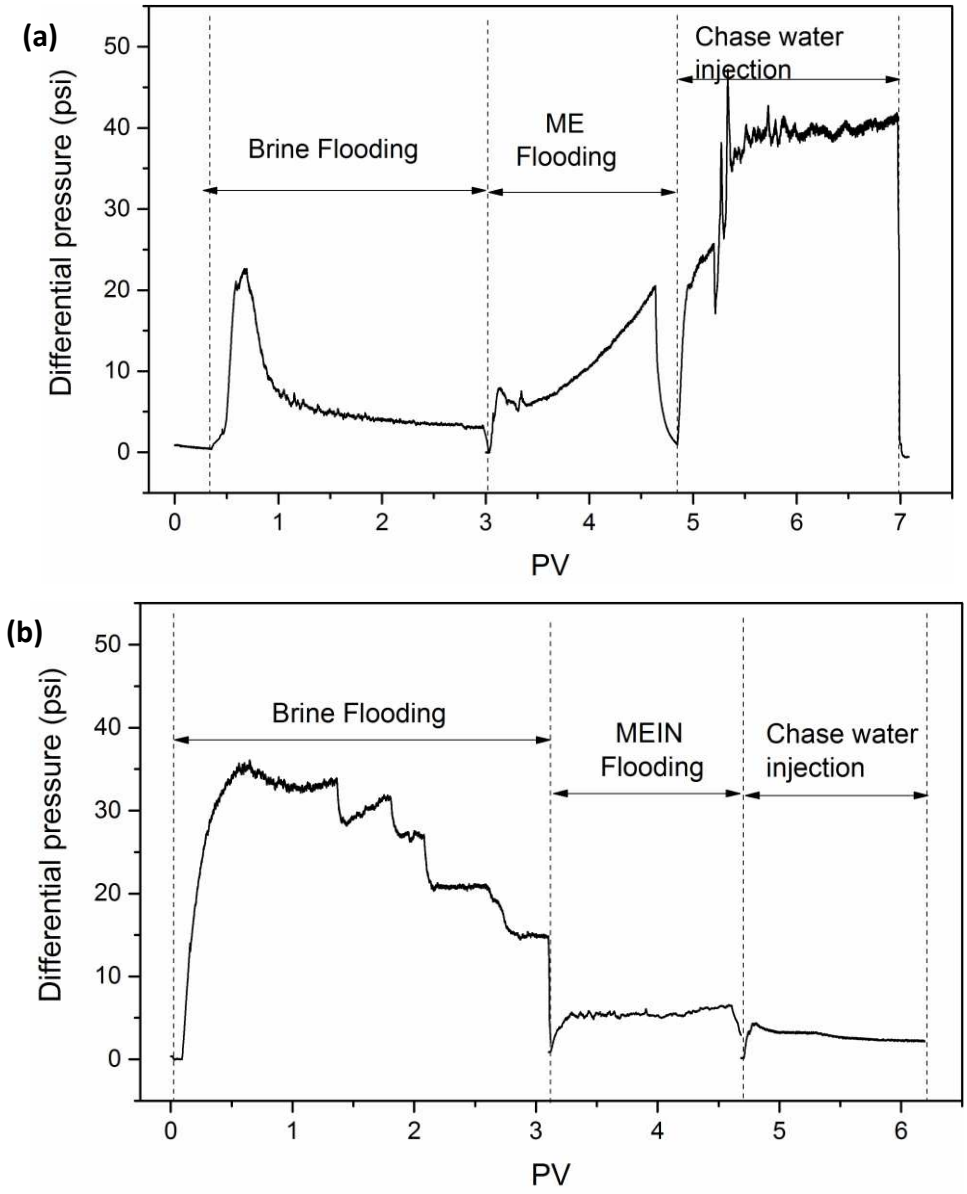

Figure 10. The differential pressure for oil displacement (a) ME, (b) MEIN with 800 ppm IONP

3.5 The mechanism for enhanced oil recovery

3.5.1 Enhanced stability by in-situ formed NPs

Although the nucleation, growth and solubility stages of nanoparticle formation may be dependent on transient dimers, collisions, and coalescence of droplets [43], the reaction itself is believed to happen at the interface since the precursor is dissolved in continuous aqueous phase [35, 44]. Moreover, particles tend to stay at o/w interface after the synthesis due to the high energy

(ΔG) required to detach the particle from the interface as calculated by the equation below (Figure 11 a). In our case, surfactant has not such complex network to trap the nanoparticle, but to form particle-surfactant joint arrangement at the interface and synergistically stabilize the ME texture (Figure 11b).

There are two main mechanisms that support the synergistic stabilization effect by NPs and surfactant: lamella drainage and hole formation [24]. We now provide a molecular-level discussion about how the in-situ synthesized NPs and surfactant synergistically stabilize the ME.

In o/w ME, aqueous lamellae separate oil droplets and prevent the droplet from coalescing, also separate the oil droplet with glass beads surface. The lamellae depends on a disjoining pressure (Π_d) originated from electrostatic, steric, structural, and additional short range repulsive forces, which counteract the van der Waals attraction between the two film surfaces [24, 45, 46]. In our case, the anionic surfactants (SDS) and the formed NPs will contribute electrostatic repulsion to Π_d (Figure 11c), and the NPs may also attribute to Π_d via structural effects that increase the osmotic pressure due to organization of particles in the lamella [47, 48], and contribute steric repulsion due to nonionic surfactant Span 80 and nanoparticle flocs 'bridging' the lamellae [49], as shown in Figure 11d.

ME may be destabilized by coalescence due to hole formation in the aqueous lamellae which separates the oil droplets. Holes appear because of thermal fluctuations that produce spatial and density variations in the film. Lamellae drainage acts to thin the aqueous lamellae, which reduces the work required to open a hole and increases the probability of hole formation [50, 51]. The nanoparticles in the present study are expected to resist bending of the interface to allow oil hole to form in lamellae. The attachment energy required to move the particle from the equilibrium

interface can be calculated by the equation below [52], in the case of pure solid particle absorbing at the interface.

$$\Delta G = \pi R^2 \gamma_{o/w} (1 \pm cos\theta)^2$$

Where, R is the particle radius. In our case, the 5-20 nm particle at the oil-water interface with surfactant lowering IFT of microscopic droplets $\gamma_{o/w}$ to 23-27 mN/m [53], would have an E equals 10^3 to 104 kT, depending on θ. It can be expected that with surfactant functionalization, particle would be unlikely detached from the interface driven by the Brownian motion. This high-level detachment energy indicates the ME system stabilized by nanoparticle is more thermodynamically stable than ME without particle. The organization of nanoparticle at the interface would provide a barrier to resist interface bending to avoid coalescence (Figure 11e). Quantitatively, bending of the interface to expose more nanoparticle to either aqueous or oil phase would be unfavorable.

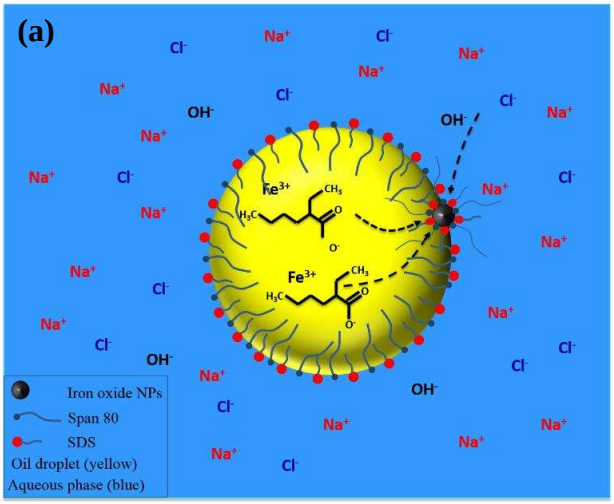

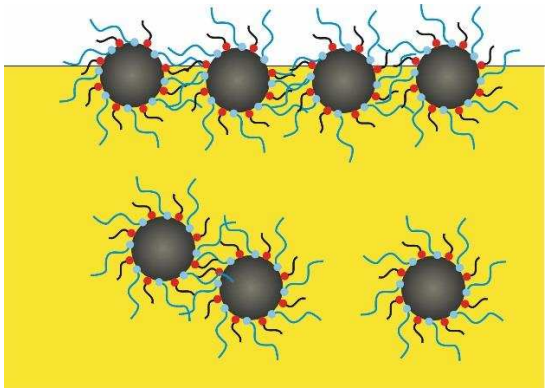

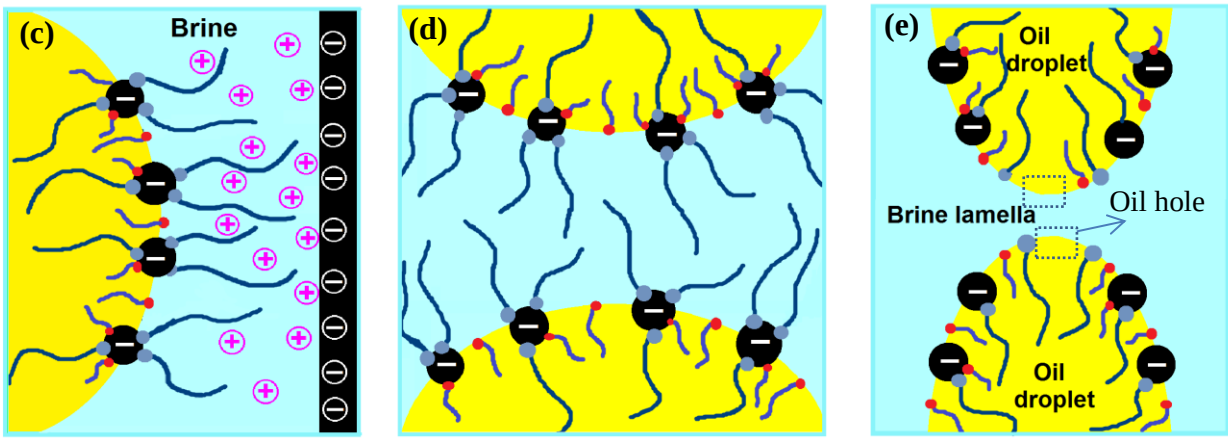

Figure 11. (a) Chemical reaction for IONP synthesis at the oil-water interface； (b) Schematic illustration of particle-surfactant joint arrangement at the interface; (c) electrostatic repulsion between ME thin film (due to the negatively-charged IONPs and anionic surfactant SDS) and negatively- charged glass beads surface, and steric effect introduced by nonionic surfactant Span 80; (d) electrostatic repulsion and steric effect between MEs thin film to counteract the van der Waals attraction to prevent them from coalescing; (e) Bending the interface to form 'oil hole' is energy unfavorable because the organization of nanoparticle at the interface would provide a barrier to resist interface bending to avoid coalescence

3.5.2 Preventing the formation of viscous Phase

Several past experimental works have shown that formation of viscous phases such as liquid crystals and viscous macroemulsions in o/w interface is a challenge for oil recovery using surfactant flooding. Viscous phase is formed when interfacial adsorption of the surfactant molecules is hindered [54]. Screening surfactants blend is a common way that is usually used for inhibiting the formation of viscous phase. For instance, branched surfactants such as twin-tailed structures are effective to minimize ordering at the o/w interface and prevent the formation of viscous phases [55, 56].

Synthesis of IONP at the interface by local chemical reaction facilitates the uniform distribution of nanoparticles, thus facilitating the attachment of surfactant molecules at the interface. Figure 12 shows that the presence of nanoparticles would prevent the formation of viscous phase at o/w interface. Therefore, a likely reason of EOR in the presence of nanoparticles in ME is the improvement of distribution of surfactant molecules at the o/w interface, so as to maintain a very low interfacial tension.

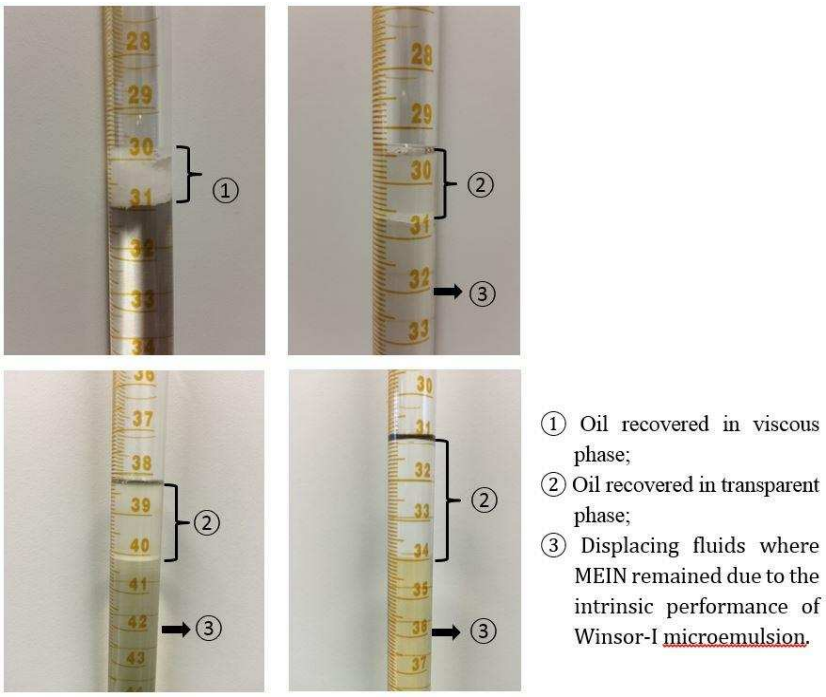

Figure 12. The oil recovered at the stage of tertiary flooding displaced by (a) ME, (b) MEIN with 800 ppm IONPs;(c) MEIN with 1600 ppm IONPs; (d) MEIN with 6400 ppm IONPs. The viscous phase formed for ME flooding, whereas the oil remained transparent state for case b to d where ME was synergistic stabilized by NPs.

3.5.3 Enhancing IFT stability

In terms of the IFT between bulk ME suspension (referring to macroscopic sample in distinguish with the IFT of microscopic emulsion droplet) and oil phase, it has been reported that the surfactant surrounding the ME would raise the chance of chromatographic separation, i.e.,

adsorption on pore surface or preferentially partitioning into the sole water or oil phase, which could cause IFT variations with possible adverse effects on oil recovery [55]. However, composition with particle allows surfactant to be more persistent at the o/w interface, thus preventing them from partitioning into water or oil phase and avoid IFT fluctuation. As shown by the dynamic IFT in the range of 0 s to 1000 s in Figure 13, it experienced significant fluctuation from around 580 s to 830 s compared to ME stabilized by NPs. Actually, the persistence of molecules at the interface has been shown to be important for emulsification and dispersion [57, 58].

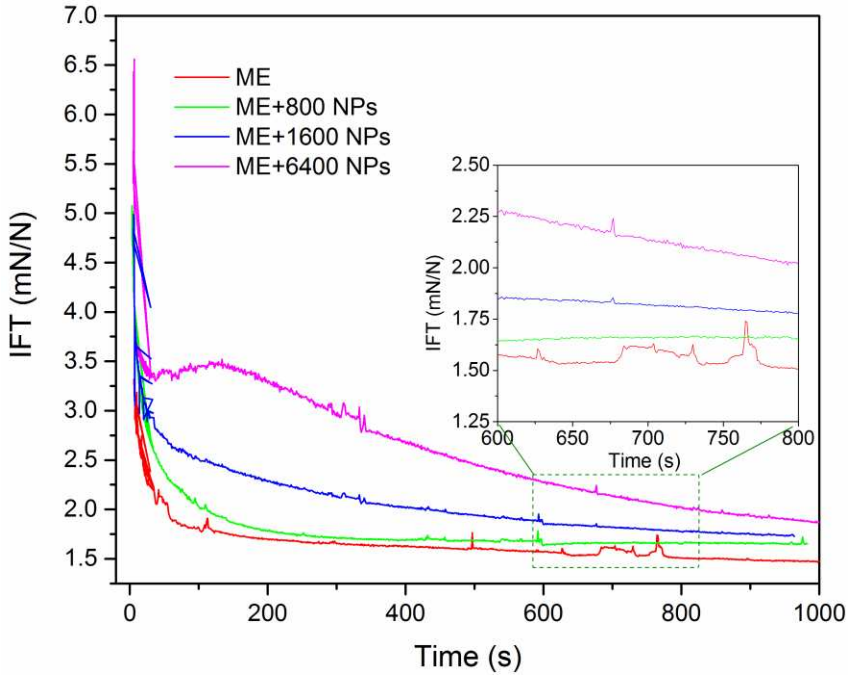

Figure 13. Dynamic viscosities between bulk ME suspension and mineral from 0 s to 1000 s for the samples applied for enhanced oil recovery, the inset is dynamic amlifying view for the dynamic viscosity changing from 600 s to 800 s.

3.5.4 Increased viscosity for mobility control

Joint arrangements of particle and surfactant at the interface could change the interfacial rheology properties. It is hypothesized here that particle-surfactant mixture could increase

interfacial elasticity and cohesiveness over particles or surfactants alone. In effect, interlocking surfactant chains between particles may act as elastic 'springs' in the layer. Also, combined effects could impart significant changes the interfacial viscosities (essentially the intrinsic hydrodynamic resistance to flow of the layer), much like increases to the bulk viscosity. Given in Figure 11b, it is a possible 'elastic' arrangement of particles and surfactant at an interface [59]. From the viscosity measurement, the formation of IONP increase the viscosity of the ME (Figure 8), which is consistent with the report by Prigiobbe et al. [42]. A synergic effect was observed between surfactant and nanoparticles on the gas viscosity, which doubled in the presence of nanoparticles. This relatively high viscosity is beneficial for the mobility control [60, 61].

4. Conclusion

This work developed a novel method to produce iron oxide nanoparticles (IONPs) in-situ in oil-in-water (o/w) MEs to increase their performance in improving oil recovery. The magnetic IONPs were synthesized in o/w ME at the optimum salinity. Core flooding experiments were carried out to evaluate oil recovery ability for MEs containing IONP at different concentrations, and possible reasons for enhanced oil recovery were analyzed. The main conclusions of the research can be summarized in the following points:

- Composite ME synergistically stabilized by surfactant and in-situ fabricated IONPs were successfully synthesized at the optimal salinity.
- Coagulating with IONPs allows the surfactant to be more persistently absorbed at the o/w interface, consequently eliminating the variation of IFT and increasing the ME viscosity.
- The synergistic stabilization effect between nanoparticle and surfactant can significantly reduce the pressure gradient and fluctuations during the flooding and post-flooding stages, due to the formation of more stable ME textures.

- Producing IONP can improve the EOR efficiency significantly. With the IONP concentration increasing from 0 to 6400 ppm, the tertiary oil recovery efficiency is boosted from 10% to 28.5% relative to OOIP, and the total oil recovery is improved remarkably from 59.1% to 85.2%.
- The oil recovery mechanism is believed mainly due to more stable ME texture synergistically stabilized by NPs and surfactants, avoiding viscous phase formation in flooding process.

5. References

[1] Schramm LL. Surfactants: Fundamentals and Applications in the Petroleum Industry. Cambridge University Press: 2010.

[2] Bera A, Kumar T, Ojha K, Mandal A. Screening of microemulsion properties for application in enhanced oil recovery. Fuel 2014; 121: 198-207.

[3] Jeirani Z, Jan B. M, Ali B. S, See C. H, Saphanuchart W. Pre-prepared Microemulsion Flooding in Enhanced Oil Recovery: A Review. Petrol Sci Technol 2014; 32(2): 180-193.

[4] Gurgel A, Moura M. C. P. A, Dantas T. N. C, Barros Neto E. L, Dantas Neto A. A. A REVIEW ON CHEMICAL FLOODING METHODS APPLIED IN ENHANCED OIL RECOVERY. Brazilian Journal of Petroleum and Gas 2008; 2: 83-95.

[5] Binks B. P, Rocher A. Effects of temperature on water-in-oil emulsions stabilised solely by wax microparticles. J Colloid Interface Sci 2009; 335(1): 94-104.

[6] Pei H. H, Zhang G. C, Ge J. J, Zhang J, Zhang Q, Fu L. P. Investigation of Nanoparticle and Surfactant Stabilized Emulsion to Enhance Oil Recovery in Waterflooded Heavy Oil Reservoirs. In: SPE Canada Heavy Oil Technical Conference, Society of Petroleum Engineers, Calgary, Alberta, Canada; 2015.

[7] Feng Y, Ye F, Liu H, Yang J. Enhancing the methanol tolerance of platinum nanoparticles for the cathode reaction of direct methanol fuel cells through a geometric design. Sci Rep 2015; 5: 16219.

[8] Zhang T, Espinosa D, Yoon K. Y, Rahmani A. R, Yu H, Caldelas F. M, Ryoo S, Roberts M, Prodanovic M, Johnston K. P, Milner T. E, Bryant S. L, Huh C. Engineered Nanoparticles as Harsh-Condition Emulsion and Foam Stabilizers and as Novel Sensors. In: Offshore Technology Conference Offshore Technology Conference, Houston, Texas, USA; 2011.

[9] Sharma T, Suresh Kumar G, Sangwai J. S. Enhanced oil recovery using oil-in-water (o/w) emulsion stabilized by nanoparticle surfactant and polymer in the presence of NaCl. Geosystem Engineering 2014; 17(3): 195-205.

[10] Zhang T, Roberts M, Bryant S. L, Huh C. Foams and Emulsions Stabilized With Nanoparticles for Potential Conformance Control Applications. In: SPE International Symposium on Oilfield Chemistry, Society of Petroleum Engineers, The Woodlands, Texas, USA. 2009.

[11] Zargartalebi M, Kharrat R, Barati N. Enhancement of surfactant flooding performance by the use of silica nanoparticles. Fuel 2015; 143: 21-27.

[12] Neves Libório De Avila J, Louise Grecco Cavalcanti De Araujo L, Drexler S, de Almeida Rodrigues J, Sandra Veiga Nascimento R. Polystyrene nanoparticles as surfactant carriers for enhanced oil recovery. J Appl Polym Sci 2016; 133(32): 43789.

[13] Saunders A. E, Koo B, Wang X, Shih C. K, Korgel B. A. Structural characterization and temperature-dependent photoluminescence of linear CdTe/CdSe/CdTe heterostructure nanorods. Chemphyschem 2008; 9(8): 1158-63.
[14] Stuart M. A, Huck W. T, Genzer J, Muller M, Ober C, Stamm M, Sukhorukov G. B, Szleifer I, Tsukruk V. V, Urban M, Winnik F, Zauscher S, Luzinov I, Minko S. Emerging applications of stimuli-responsive polymer materials. Nat Mater 2010; 9(2): 101-13.
[15] Makaram P, Selvarasah S, Xiong X, Chen C. L, Busnaina A, Khanduja N, Dokmeci M. R. Three-dimensional assembly of single-walled carbon nanotube interconnects using dielectrophoresis. Nanotechnology 2007; 18(39): 395204.
[16] Wright S. A, Gianchandani Y. B. Discharge-Based Pressure Sensors for High-Temperature Applications Using Three-Dimensional and Planar Microstructures. J Microelectromech Syst 2009; 18(3): 736-743.
[17] Korgel B. A. Semiconductor nanowires: A chemical engineering perspective. AlChE J 2009; 55(4): 842-848.
[18] Dirmyer M. R, Martin J, Nolas G. S, Sen A, Badding J. V. Thermal and electrical conductivity of size-tuned bismuth telluride nanoparticles. Small 2009; 5(8): 933-7.
[19] Gao H, Wen D, Tarakina N. V, Liang J, Bushby A. J, Sukhorukov G. B. Bifunctional ultraviolet/ultrasound responsive composite TiO2/polyelectrolyte microcapsules. Nanoscale 2016; 8(9): 5170-80.
[20] Gao H, Wen D. S, Sukhorukov G. B. Composite silica nanoparticle/polyelectrolyte microcapsules with reduced permeability and enhanced ultrasound sensitivity. J Mater Chem B 2015; 3(9): 1888-1897.
[21] Prodanovic M.; Ryoo S.; Amir R. Rahmani Roman Kuranov Csaba Kotsmar Effects of Magnetic Field on Paramagnetic Nanoparticles in Porous Media Effects of Magnetic Field on the Motion of Multiphase Fluids Containing Paramagnetic Nanoparticles in Porous Media. In: 2010 SPE Improved Oil Recovery Symposium, Tulsa, Oklahoma, USA; 2010.
[22] Huh C, Bryant S. L, Milner T. E, Johnston K. P, Yoon K. Y, Bielawski C. Determination of oil saturation in reservoir rock using paramagnetic nanoparticles and magnetic field. In: Google Patents; 2011.
[23] Sun Q, Li Z, Li S, Jiang L, Wang J, Wang P. Utilization of Surfactant-Stabilized Foam for Enhanced Oil Recovery by Adding Nanoparticles. Energy Fuels 2014; 28(4): 2384-2394.
[24] Worthen A. J, Bryant S. L, Huh C, Johnston K. P. Carbon dioxide-in-water foams stabilized with nanoparticles and surfactant acting in synergy. AlChE J. 2013; 59(9): 3490-3501.
[25] Aroonsri A, Worthen A. J, Hariz T, Johnston K. P, Huh C, Bryant S. L. Conditions for Generating Nanoparticle-Stabilized CO2 Foams in Fracture and Matrix Flow. In: SPE Annual Technical Conference and Exhibition, Society of Petroleum Engineers, New Orleans, Louisiana, USA; 2013.
[26] Gupta A, Eral HB, Hatton TA, Doyle PS. Nanoemulsions: formation properties and applications. Soft Matter 2016; 12(11): 2826-41.
[27] Gupta A, Eral HB, Hatton TA, Doyle PS. Controlling and predicting droplet size of nanoemulsions: scaling relations with experimental validation. Soft Matter 2016; 12(5): 1452-8.
[28] Binks BP, Rodrigues JA. Enhanced stabilization of emulsions due to surfactant-induced nanoparticle flocculation. Langmuir 2007; 23(14): 7436-9.
[29] Flaaten A, Nguyen QP, Pope GA, Zhang J. A Systematic Laboratory Approach to Low-Cost High-Performance Chemical Flooding. SPE Reservoir Evaluation & Engineering 2008; 12(05): 713-723.
[30] Flaaten A. K. An Integrated Approach to Chemical EOR Opportunity Valuation: Technical Economic and Risk Considerations for Project Development Scenarios and Final Decision. The University of Texas at Austin 2012.
[31] Wang Y, Li Y, Fortner J. D, Hughes J. B, Abriola L. M, Pennell K. D. Transport and retention of nanoscale C60 aggregates in water-saturated porous media. Environ Sci Technol 2008; 42(10): 3588-94.
[32] Shani C, Weisbrod N, Yakirevich A. Colloid transport through saturated sand columns: Influence of physical and chemical surface properties on deposition. Colloids Surf. A 2008; 316(1-3): 142-150.

[33] Yoon J. S, Germaine J. T, Culligan P. J. Visualization of particle behavior within a porous medium: Mechanisms for particle filtration and retardation during downward transport. Water Resour Res 2006; 42(6): W06417.
[34] Wang C, Bobba A. D, Attinti R, Shen C, Lazouskaya V, Wang L. P, Jin Y. Retention and transport of silica nanoparticles in saturated porous media: effect of concentration and particle size. Environ Sci Technol 2012; 46(13): 7151-7158.
[35] Okoli C, Sanchez-Dominguez M, Boutonnet M, Jaras S, Civera C, Solans C, Kuttuva G. R. Comparison and functionalization study of microemulsion-prepared magnetic iron oxide nanoparticles. Langmuir 2012; 28(22): 8479-85.
[36] Sanchez-Dominguez M, Pemartin K, Boutonnet M. Preparation of inorganic nanoparticles in oil-in-water microemulsions: A soft and versatile approach. Curr Opin Colloid Interface Sci 2012; 17(5): 297-305.
[37] Sanchez-Dominguez M, Koleilat H, Boutonnet M, Solans C. Synthesis of Pt Nanoparticles in Oil-in-Water Microemulsions: Phase Behavior and Effect of Formulation Parameters on Nanoparticle Characteristics. J Dispersion Sci Technol 2011; 32(12): 1765-1770.
[38] Murray B. S, Durga K, Yusoff A, Stoyanov S. D. Stabilization of foams and emulsions by mixtures of surface active food-grade particles and proteins. Food Hydrocoll 2011; 25(4): 627-638.
[39] Lishchuk S. V, Halliday I. Effective surface viscosities of a particle-laden fluid interface. Phys Rev E Stat Nonlin Soft Matter Phys 2009; 80(1 Pt 2): 016306.
[40] Wijmans C. M, Dickinson E. Simulation of Interfacial Shear and Dilatational Rheology of an Adsorbed Protein Monolayer Modeled as a Network of Spherical Particles. Langmuir 1998; 14(25): 7278-7286.
[41] Kabalnov A, Wennerström H. Macroemulsion Stability: The Oriented Wedge Theory Revisited. Langmuir 1996; 12(2): 276-292.
[42] Prigiobbe V, Worthen A. J, Johnston K. P, Huh C, Bryant S. L. Transport of Nanoparticle-Stabilized CO2-Foam in Porous Media. Transport Porous Med 2015; 111(1): 265-285.
[43] Destree C, Nagy J. B. Mechanism of formation of inorganic and organic nanoparticles from microemulsions. Adv Colloid Interface Sci 2006; 123: 353-367.
[44] Nourafkan E, Asachi M, Gao H, Raza G, Wen D. Synthesis of stable iron oxide nanoparticle dispersions in high ionic media. Ind Eng Chem Res 2017; 50: 57-71.
[45] Adkins S. S, Chen X, Chan I, Torino E, Nguyen Q. P, Sanders A. W, Johnston K. P. Morphology and stability of CO2-in-water foams with nonionic hydrocarbon surfactants. Langmuir 2010; 26(8): 5335-48.
[46] Wasan D, Nikolov A, Kondiparty K. The wetting and spreading of nanofluids on solids: Role of the structural disjoining pressure. Curr Opin Colloid Interface Sci 2011; 16(4): 344-349.
[47] Wasan D, Nikolov A. Thin liquid films containing micelles or nanoparticles. Curr Opin Colloid Interface Sci 2008; 13(3): 128-133.
[48] Langevin D. Influence of interfacial rheology on foam and emulsion properties. Adv Colloid Interface Sci 2000; 88(1-2): 209-222.
[49] Binks B. P, Kirkland M, Rodrigues J. A. Origin of stabilisation of aqueous foams in nanoparticle–surfactant mixtures. Soft Matter 2008; 4(12): 2373.
[50] Vrij A, Overbeek J. T. G. Rupture of thin liquid films due to spontaneous fluctuations in thickness. J Am Chem Soc 1968; 90(12): 3074-3078.
[51] Babak V. G, Stébé M.-J. Highly Concentrated Emulsions: Physicochemical Principles of Formulation. J Dispersion Sci Technol 2002; 23(1-3): 1-22.
[52] Binks B. P, Lumsdon S. O. Influence of Particle Wettability on the Type and Stability of Surfactant-Free Emulsions. Langmuir 2000; 16(23): 8622-8631.
[53] Martinez H, Chacon E, Tarazona P, Bresme F. The intrinsic interfacial structure of ionic surfactant monolayers at water-oil and water-vapour interfaces. Proc R Soc A 2011; 467(2131): 1939-1958.
[54] Fanun M. Microemulsions: Properties and Applications. CRC Press: 2008.
[55] Hirasaki G, Miller C. A, Puerto M. Recent Advances in Surfactant EOR. SPE Journal 2011; 16(04): 889-907.

[56] Barnes J. R, Groen K, On A, Dubey S. T, Reznik C, Buijse M. A, Shepherd A. G. Controlled Hydrophobe Branching To Match Surfactant To Crude Composition For Chemical EOR. In: SPE Improved Oil Recovery Symposium, Society of Petroleum Engineers, Tulsa, Oklahoma, USA; 2012.
[57] Boyd J, Parkinson C, Sherman P. Factors affecting emulsion stability and the HLB concept. J Colloid Interface Sci 1972; 41(2): 359-370.
[58] Riehm D. A, McCormick A. V. The role of dispersants' dynamic interfacial tension in effective crude oil spill dispersion. Mar Pollut Bull 2014; 84(1-2): 155-63.
[59] Hunter T. N, Pugh R. J, Franks G. V, Jameson G. J. The role of particles in stabilising foams and emulsions. Adv Colloid Interface Sci 2008; 137(2): 57-81.
[60] ShamsiJazeyi H, Miller C. A, Wong M. S, Tour J. M, Verduzco R. Polymer-Coated Nanoparticles for Enhanced Oil Recovery. J Appl. Polym Sci 2014; 131(15): 40576.
[61] Raffa P, Broekhuis A. A, Picchioni F. Polymeric surfactants for enhanced oil recovery: A review. J Petrol Sci Eng 2016; 145: 723-733.